JOURNAL OF GEOPHYSICAL RESEARCH, VOL. 100, NO. D12, PAGES 26,105–26,116, DECEMBER 20, 1995

Direct shortwave forcing of climate by the anthropogenic sulfate aerosol: Sensitivity to particle size, composition, and relative humidity

Seth Nemesure, Richard Wagener, and Stephen E. Schwartz

Environmental Chemistry Division, Brookhaven National Laboratory, Upton, New York

Abstract. Recent estimates of global or hemispheric average forcing of climate by anthropogenic sulfate aerosol caused by scattering of shortwave radiation ("direct" effect) are uncertain by somewhat more than a factor of 2. The principal sources of this uncertainty are atmospheric chemistry properties (yield, residence time), and microphysical properties (scattering efficiency, upscatter fraction, and the dependence of these properties on particle size, composition, and relative humidity, (RH)). This paper examines the sensitivity of forcing to these microphysical properties to identify and improve understanding of the properties required to reduce the uncertainty in the forcing. The relations between aerosol loading and forcing developed here are suitable for comparing modeled and measured aerosol forcing at specific locations and for use in climate models, provided aerosol composition and microphysical properties are known, calculated, or assumed. Results are presented showing the dependence of scattering efficiency, upscatter fraction, and normalized forcing (W $m^{-2}/g(SO_4^{2-})$ m^{-2} or W $g(SO_4^{2-})^{-1}$) on dry particle size (expressed as mole(sulfate) per particle), composition ($(NH_4)_2SO_4$, NH_4HSO_4, H_2SO_4), solar zenith angle, latitude, and season. Forcing is strongly dependent on dry particle size and RH but is relatively insensitive to composition. The normalized forcing can be integrated over a known or assumed size distribution to evaluate the sulfate aerosol forcing. Global and annual average values of the normalized forcing are evaluated as a function of particle size and RH. Depending on values of these variables, normalized forcing may be less than, intermediate to, or greater than the range of previous estimates of sulfate aerosol forcing.

1. Introduction

Radiative forcing of climate by anthropogenic aerosols is thought to be a major contributor to the changing radiative balance of the Earth-atmosphere system. Light scattering by aerosols under cloud-free conditions (direct effect) and an enhanced brightness of clouds caused by an increased concentration of cloud condensation nuclei (indirect effect) are the key processes that have been identified [*Twomey et al.*, 1984; *Schwartz*, 1988, 1995; *Charlson et al.*, 1990, 1991, 1992; *Penner et al.*, 1992, 1994; *Wigley and Raper*, 1992; *Kiehl and Briegleb*, 1993; *Boucher and Anderson*, 1995; *Haywood and Shine*, 1995].

This paper examines factors governing the magnitude of the direct effect by anthropogenic sulfates. Among anthropogenic aerosols much attention has been focused on sulfates because of their importance and because of knowledge of their distribution and properties that permits quantitative evaluation. *Charlson et al.*, [1990, 1992] and *Penner et al.* [1994] have estimated the magnitude of the direct forcing using a box model as a first approximation. This approximation is reasonable on global average given that the forcing is linear in aerosol loading in the optically thin limit. Box models readily allow for examination of uncertainties but cannot account for geographic distribution, for which a chemical transport model is required [*Charlson et al.*, 1991; *Taylor and Penner*, 1994]. Box model calculations to date also have not taken into account the wavelength dependence of aerosol and Rayleigh scattering [*Kiehl and Briegleb*, 1993], but this is not an inherent limitation. More importantly, box models cannot account for correlation among the several controlling variables. Nonetheless, box models continue to lend great insight into aerosol forcing of climate.

The box model expression for global average shortwave forcing for a hypothetical cloud-free planet for a specific loading of atmospheric sulfate is [*Charlson et al.*, 1992]

$$\Delta F_{SO_4^{2-}} = -\frac{1}{2} F_T T^2 (1 - R_s)^2 \overline{\beta} \alpha^{RH_r}_{SO_4^{2-}} \mathcal{F}(RH) B_{SO_4^{2-}} \quad (1)$$

The minus sign indicates that this forcing exerts a cooling influence, and the factor $\frac{1}{2}$ is due to the fact that

Copyright 1995 by the American Geophysical Union.

Paper number 95JD02897.
0148-0227/95/95JD-02897$05.00

only half the planet is illuminated at any given period of time. The symbols in the above equation are defined as follows:

F_T = the solar constant, the solar radiative flux at a mean distance from the Earth to the Sun;

T = the fraction of incident or scattered light transmitted through the atmosphere above the aerosol layer. The factor T^2 takes into account transmittance of incident and scattered radiation;

R_s = the albedo of the underlying surface. The factor $(1 - R_s)^2$ takes into account multiple reflection between the surface and the aerosol layer;

$\overline{\beta}$ = the fraction of the radiation scattered upward by the aerosol, averaged over the sunward hemisphere of the planet;

$\alpha_{SO_4^{2-}}^{RH_r}$ = the light-scattering efficiency of sulfate aerosol, that is, scattering coefficient per sulfate mass, at a reference low relative humidity, RH, commonly taken as RH_r = 30%;

$\mathcal{F}(RH)$ = the increase in scattering cross section at ambient RH relative to that at the reference RH; and

$B_{SO_4^{2-}}$ = the average sulfate column mass burden, evaluated as the product of the source strength of anthropogenic SO_2, the fractional yield of emitted SO_2 that reacts to produce sulfate aerosol, and the mean residence time of SO_2 aerosol in the atmosphere divided by the area of the geographical region to which the calculation is applied.

To evaluate forcing for the actual planet, an additional factor (1-A_c) (A_c is the fractional cloud cover) must be included in (1) because the albedo enhancement applies mainly to cloud-free regions [*Charlson et al.*, 1992], although a significant contribution may also be expected from cloud-covered regions [*Boucher and Anderson*, 1995].

Recent box model estimates of global average direct forcing of climate by anthropogenic sulfate are about -1 W m^{-2} [*Charlson et al.*, 1992; *Penner et al.*, 1994], uncertain to a factor of somewhat greater than 2; estimates of forcing based on the geographically distributed aerosol are somewhat lower [*Kiehl and Briegleb*, 1993; *Boucher and Anderson*, 1995] in part because of lower values of mean sulfate burden employed in those estimates. These estimates thus indicate that the direct effect of anthropogenic sulfate exerts a forcing on climate comparable in magnitude (but opposite in sign) to the forcing produced by anthropogenic enhancement of greenhouse gas concentrations. The principal sources of uncertainty in these estimates are atmospheric chemistry properties (yield, residence time), and microphysical properties that influence optical and radiative properties of the aerosol (scattering efficiency, upscatter fraction, including dependence on particle size, composition, and RH) [*Hegg et al.*, 1993; *Penner et al.*, 1994; *IPCC*, 1994; *Haywood and Shine*, 1995; *Boucher and Anderson*, 1995]. The uncertainty in aerosol forcing generally, and sulfate forcing in particular, greatly limits present knowledge of the net anthropogenic influence on the Earth radiation budget over the industrial period [*IPCC*, 1994].

In order to isolate sources of uncertainty, it is useful to represent this forcing normalized to the sulfate loading. To focus on the radiative terms in (1), we define normalized forcing for a cloud-free region as

$$\Delta G_{SO_4^{2-}} = \frac{\Delta F_{SO_4^{2-}}}{B_{SO_4^{2-}}}, \tag{2}$$

a quantity which has units of W m^{-2} per g(SO_4^{2-}) m^{-2}, or W g(SO_4^{2-})$^{-1}$. This quantity has previously been introduced by *Boucher and Anderson* [1995] and was denoted by them as a climate forcing efficiency. On the basis of the global and annual values given by *Charlson et al.* [1992], $\overline{\Delta G} = -715$ W g(SO_4^{2-})$^{-1}$ for a cloud-free planet. The corresponding quantity for the geographically distributed forcing calculation of *Kiehl and Briegleb* [1993] ranges from -180 to -290 W g(SO_4^{2-})$^{-1}$, depending on dry particle radius [*Boucher and Anderson*, 1995]. For their own geographically distributed forcing calculation *Boucher and Anderson* [1995] obtained $\overline{\Delta G}$ ranging from -160 to -250 W g(SO_4^{2-})$^{-1}$, again depending on the value of dry particle radius employed. Although, as discussed below, some of the reasons for these differences are understood, there is still a substantial range of uncertainty reflected in the different values of normalized forcing represented by these several results. As noted by *Charlson et al.* [1992] and *Penner et al.* [1994], about a third of the overall uncertainty in sulfate direct forcing is associated with the several optical/radiative properties of aerosols appearing in (1): the light scattering efficiency per unit sulfate mass ($\alpha_{SO_4^{2-}}^{RH_r}$), the increase in light scattering as a function of RH ($\mathcal{F}$(RH)), and the fraction of scattered light which is scattered into the upward hemisphere (β). Each of these quantities varies substantially with particle size and wavelength and perhaps also with chemical form. It is well known that particle size is a strong function of RH [*Garland*, 1969; *Tang and Munkelwitz*, 1977, 1994; *Hegg et al.*, 1993] because of the deliquescent/hygroscopic nature of water-soluble aerosols, and as a consequence the optical properties must also be scaled according to *RH* [*Charlson et al.*, 1992; *Kiehl and Briegleb*, 1993]. Recently, *Kaufman and Holben* [in press, 1995] have called attention to the dependence of upscatter fraction on aerosol size distribution and the sensitivity of forcing to the sulfate variability in upscatter fraction.

This paper examines the dependencies of optical and radiative properties of sulfate aerosols on microphysics and composition that go into evaluation of the direct forcing given by (1). Three particle compositions are considered, ammonium sulfate ($(NH_4)_2SO_4$), ammonium bisulfate (NH_4HSO_4), and sulfuric acid (H_2SO_4), taking into account the hygroscopic properties of these materials. In order to explicitly examine the influence of RH, we define the wet scattering efficiency relative to the mass of sulfate in the aerosol as

$$\alpha^* = \alpha_{SO_4^{2-}}^{RH_r} \cdot \mathcal{F}(RH). \quad (3)$$

The light scattering properties α^* and β are computed as functions of radius and composition and, in the case of β, solar zenith angle (SZA) and season. A Mie scattering model is used to derive the optical properties of the given compositions, dry particle size and RH, and a doubling and adding multiple scattering model is used to compute a seasonal, latitudinal, and daily distribution of the forcing by particles of each of these compositions. The global and annual values of the aerosol forcing are then calculated as a function of particle dry radius and for representative size distributions and compared to the values given by *Charlson et al.* [1992], *Kiehl and Briegleb* [1993], and *Boucher and Anderson* [1995].

2. Methods

The Mie scattering model of *Hansen and Travis* [1974] was used to determine $\alpha^*(\lambda)$ and the phase function $P_{a,\lambda}(\theta)$, where θ = scattering angle. We chose a gamma particle size distribution (effective variance equal to 0.01) wide enough to remove any resonances in the particle size range considered, yet narrow enough that the Mie scattering properties were calculated essentially for monodisperse aerosols. For actual (polydisperse) aerosols, derived radiative quantities may readily be evaluated by appropriate integration over particle radius. The refractive index is assumed to be real, that is, no absorption ($n = n_r - in_i$ where $n_i = 0$). For weakly absorbing particles ($n_i \ll 1$) the scattering properties differ negligibly from those of purely scattering particles [*Twomey*, Elsevier, New York, 1977].

The spectral dependence of aerosol forcing was treated by a radiative transfer model that divided the spectrum into seven intervals from 0.3 to 1.0 μm. All the scattering was assumed to take place within this spectral range, for which the atmosphere is assumed to be nonabsorbing; that is, all of the atmospheric absorption (30%) is assumed to take place shortward of 0.3 μm (ozone) and longward of 1.0 μm (water vapor) [*Coakley et al.*, 1983]. The contributions of the incident solar radiation and the Rayleigh optical depths at each of these wavelengths are summarized in Table 1. Scattering at wavelengths greater than 1.0 μm is neglected because of the low top-of-atmosphere power, the relatively high atmospheric absorption, and the reduced scattering cross section in this wavelength region. The enhancement in spectral power in the 0.3 to 1.0 μm band caused by neglect of atmospheric absorption largely compensates the scattering at wavelengths greater than 1.0 μm. This treatment may lead to a slight overestimate in scattering because of the greater scattering cross section at shorter wavelengths. *Boucher and Anderson's* [1995] values are about 20% lower, perhaps because they averaged over the entire solar spectrum, which includes some contribution from wavelengths above 1.0 μm.

Table 1. Representation of Solar Spectrum Used in Calculations [*Coakley et al.*, 1983]

λ, Wavelength, μm	f_λ, Fraction of Incident Solar Flux	τ_r, Rayleigh Optical Depth
0.340	0.0579	0.6853
0.434	0.1389	0.2532
0.508	0.0561	0.1332
0.550	0.1527	0.0964
0.768	0.1342	0.0247
0.833	0.0881	0.0178
0.991	0.0704	0.0087

The radiative transfer was computed using a doubling and adding multiple scattering model [*Hansen and Travis*, 1974]. The model is based on the fact that if reflection and transmission are known for two layers in the atmosphere, then the resultant reflection and transmission of the two layers can be obtained by computing the successive orders of scattering between the two layers. Here we assumed that the surface is Lambertian ($R_s = 0.15$), and the atmosphere was treated as consisting of a homogeneously mixed layer with Rayleigh scattering and aerosol scattering. The combined Rayleigh and aerosol phase function was computed using an expression weighted by the Rayleigh (r) and aerosol (a) optical depths

$$P_\lambda(\theta) = \frac{\tau_{a,\lambda} P_{a,\lambda}(\theta) + \tau_{r,\lambda} P_{r,\lambda}(\theta)}{\tau_{a,\lambda} + \tau_{r,\lambda}}. \quad (4)$$

The model output is a local plane albedo that varies with the aerosol optical depth τ_a and the aerosol scattering phase function $P_{a,\lambda}(\theta)$ and is a function of SZA (θ_0) and wavelength (λ).

The aerosol forcing at each of the seven wavelengths, ΔF_λ, was evaluated as the difference between top-of-atmosphere net flux for two calculations, with aerosol optical depth at $\lambda = 0.508$ μm of 0.10 and 0.05. These values represent the effect of incremental anthropogenic sulfate of optical depth 0.05 at 0.508 μm superimposed on a background aerosol of optical depth 0.05 [*Forgan*, Australia, 1987]. The total shortwave forcing as a function of the $\cos(\theta_0)$, μ_0, is given by the weighted sum

$$\Delta F(\mu_0) = \sum_\lambda f_\lambda \Delta F_\lambda(\mu_0), \quad (5)$$

where the fractional solar flux f_λ is given in Table 1.

Although in a conservatively scattering atmosphere, the normalized forcing is independent of the vertical

distribution of the scattering particles [*Coakley et al.*, 1983, their Appendix A], the functional dependence of local plane albedo on SZA depends somewhat on the vertical distribution of the aerosol. In the real world, this vertical distribution is somewhere between the homogeneous distribution used in our calculations and a distribution that confines the aerosol entirely to the atmospheric boundary layer. In order to bound the dependence on aerosol vertical distribution, the direct aerosol forcing was also evaluated for a model atmosphere that consisted of a boundary layer from 1000 to 700 hPa containing the same optical depth of aerosol scattering as in the homogeneous case, with an overlaying aerosol-free upper troposphere/stratosphere layer above 700 hPa. The result for a representative dry particle radius ($R = 0.11$ μm), RH (80%), and composition ($(NH_4)_2SO_4$) showed a slight (7%) increase in normalized forcing at $\mu_0 = 1$ (overhead sun), and slight decrease (2%) at $\mu_0 < 0.5$, relative to the one-layer model. Such a dependence on the vertical distribution is of no consequence for the present analysis.

The instantaneous normalized clear-sky forcing was obtained by dividing by the sulfate mass burden;

$$\Delta G(\mu_0) = \frac{\Delta F(\mu_0)}{B_{SO_4^{2-}}}, \tag{6}$$

where the sulfate mass burden $B_{SO_4^{2-}}$ is that which corresponds at the RH of the calculation to an aerosol optical depth of 0.05 at $\lambda = 0.508$ μm. The diurnal (24-hour) average normalized forcing was evaluated as $\frac{1}{T}\int \Delta G(\mu_0(t))dt$. The global average value was evaluated as

$$\overline{\Delta G} = \frac{1}{4\pi}\int_0^{2\pi} d\phi_0 \int_0^{\frac{\pi}{2}} \Delta G(\cos\theta_0)\sin\theta_0 d\theta_0 = \frac{1}{2}\int_0^1 \Delta G(\mu_0)d\mu_0 \tag{7}$$

where ϕ_0 is the azimuth of the SZA; that is, half the average over the illuminated hemisphere. Integration of the diurnal average forcing over latitude and season yielded essentially identical results.

3. Results

3.1. Scattering Efficiency

Composition and index of refraction as functions of RH for $(NH_4)_2SO_4$, NH_4HSO_4, and H_2SO_4 are given in *Tang and Munkelwitz* [1994] and *Weast and Astle* [The Chemical Rubber Co., Ohio, 63 ed., 1982]. The RH dependence of particle radius R relative to dry radius R_0 is shown in Figure 1; the refractive indices for the three compositions as a function of RH are shown in Figure 2. Figure 1 shows a substantial increase in particle radius associated with hygroscopic growth above the deliquescence point, that is, the RH corresponding to the vapor pressure of water above a saturated solution indicated by the vertical lines shown for $(NH_4)_2SO_4$ and NH_4HSO_4. In the case of H_2SO_4 the compound undergoes no phase transition, remaining a liquid throughout the entire range of RH. (Surface tension contributes only a 5% error in particle size for a wet particle radius of 0.025 μm decreasing with larger particle sizes, and consequently this effect is ignored in the present study.) Note that for $(NH_4)_2SO_4$ and NH_4HSO_4 the graphs for R/R_0 (and also for index of refraction, Figure 2) extend to RH well below the deliquescence points of these materials. Aerosols in the laboratory [*Tang and Munkelwitz*, 1994] and in the ambient atmosphere [*Rood et al.*, 1989] remain as supersaturated liquids at RH's well below the deliquescence point, (crystallization humidities $\sim$ 39% for $(NH_4)_2SO_4$; 3% for NH_4HSO_4), and it is thus probably appropriate for the most part to evaluate their light scattering properties as solutions rather than crystallized salts. We therefore assume that sulfate particles are always hydrated for RH

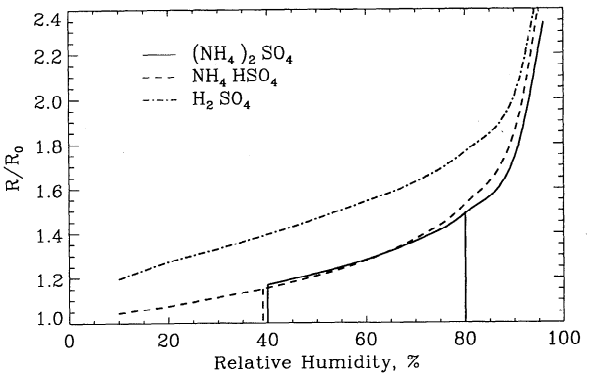

Figure 1. Dependence of particle size on relative humidity for ammonium sulfate ($(NH_4)_2SO_4$), ammonium bisulfate (NH_4HSO_4) and sulfuric acid (H_2SO_4). The data were obtained from *Tang and Munkelwitz* [1994]. Solid vertical lines denote the efflorescence and deliquescence relative humidity RH for ammonium sulfate. The dashed line represents the deliquescence RH for ammonium bisulfate. The efflorescence point for ammonium bisulfate is at RH $\approx$ 2.5% and is not shown.

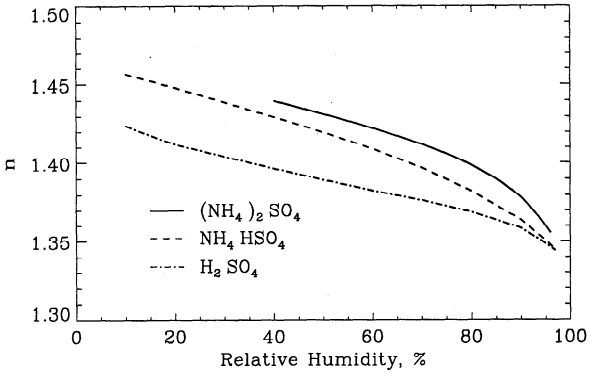

Figure 2. Refractive index versus relative humidity for three particle compositions, $(NH_4)_2SO_4$, NH_4HSO_4, and H_2SO_4 (data from *Tang and Munkelwitz* [1994]).

above their crystallization humidities. *Boucher and Anderson* [1995] showed that this assumption gives an 18% higher forcing for ammonium sulfate than if they are always crystallized, for 40% < RH < 80%. Thus any overestimation of the forcing is bounded by this value, and is probably only a few percent at most.

The fact that RH plays a major role in determining the size of the particle implies that RH will also significantly influence the light scattering efficiency, α^*. The dependence of the scattering efficiency on particle size and composition is shown in Figure 3. Here the primary label on the abscissa represents the amount of sulfate (moles) per particle of sulfate, $N_{SO_4^{2-}}$; the secondary axes denote the more familiar particle dry radius, evaluated as

$$R_0 = \left(\frac{3 N_{SO_4^{2-}} M}{4\pi\rho} \right)^{\frac{1}{3}} \quad (8)$$

where R_0 is the dry particle radius, ρ is the density, and M is the molecular weight of the compound. In the case of H_2SO_4 the dry radius is taken at RH = 0. The ordinate represents the light scattering efficiency of the wet particle per sulfate mass, that is, the quantity α^*. It is seen from this figure that the scattering efficiency varies considerably with the amount of sulfate in the particle for a given RH. At each RH, α^* exhibits a characteristic maximum corresponding roughly to the coincidence of particle diameter with wavelength. For any given dry radius, α^* increases strongly with increasing RH. For example, for $(NH_4)_2SO_4$, the scattering efficiency reaches a maximum of $\sim$ 8 m^2 g$(SO_4^{2-})^{-1}$ at RH = 40%, $\sim$ 15 m^2 g$(SO_4^{2-})^{-1}$ at RH = 80%, $\sim$ 25 m^2 g$(SO_4^{2-})^{-1}$ at RH = 90% and $\sim$ 65 m^2 g$(SO_4^{2-})^{-1}$ at RH = 97%. This high sensitivity of α^* to RH together with the highly variable and not well-characterized global distribution of RH accounts for much of the uncertainty in direct forcing by sulfate ascribed by *Penner et al.* [1994] to the RH factor $\mathcal{F}$.

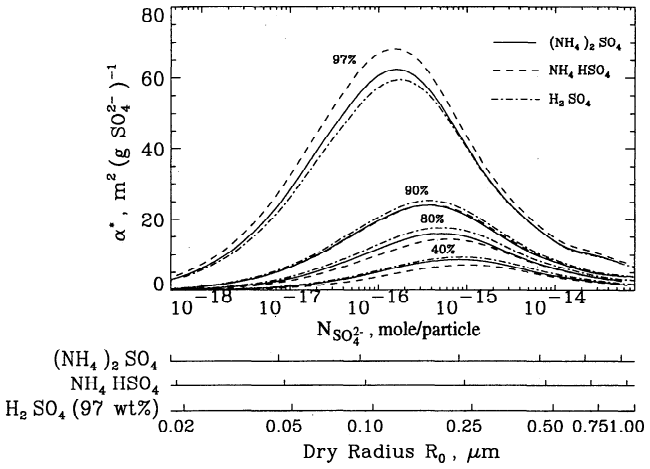

Figure 3. Dependence of scattering efficiency for aqueous $(NH_4)_2SO_4$, NH_4HSO_4, and H_2SO_4 aerosol on dry particle size expressed as amount of substance per particle $N_{SO_4^{2-}}$ for indicated values of RH, averaged over the solar spectrum. Particle dry radius, R_0 (evaluated as the radius of the sphere of equal volume) is also shown by means of the secondary axes

The values of α^* in Figure 3 may be compared to the quantity $\alpha\mathcal{F}(RH)$ = 8.5 m^2 g$(SO_4^{2-})^{-1}$ employed in the evaluation by *Charlson et al.* [1992], for α = 5 m^2 g$(SO_4^{2-})^{-1}$ and $\mathcal{F}(RH)$ = 1.7. The *Charlson et al.* [1992] value of $\alpha\mathcal{F}(RH)$ corresponds to a wavelength of 0.55 μm which, as noted by *Kiehl and Briegleb* [1993], leads to an overestimate of the actual value that corresponds to the solar spectrum. The wavelength dependence of α^* is shown in Figure 4 for several values of RH, confirming the decrease with increasing wavelength noted by *Kiehl and Briegleb* [1993]. Despite this wavelength dependence, the values for α^* shown in Figure 3, which are averages over the solar spectrum, indicate that the *Charlson et al.* [1992] value of 8.5 m^2 g$(SO_4^{2-})^{-1}$ may well be an underestimate, depending on the actual particle size distribution and RH.

3.2. Upscatter Fraction

Following *Wiscombe and Grams* [1976], we denote the upscatter fraction, β, as the portion of light scattered by an aerosol that is scattered into the upward hemisphere relative to the local horizon. It is this upward scattered fraction, and not the back scattered fraction, that is pertinent to radiative forcing by aerosol single scattering. Upscatter fraction depends on the SZA as well as on the angular distribution of the light scattering by the aerosol (phase function).

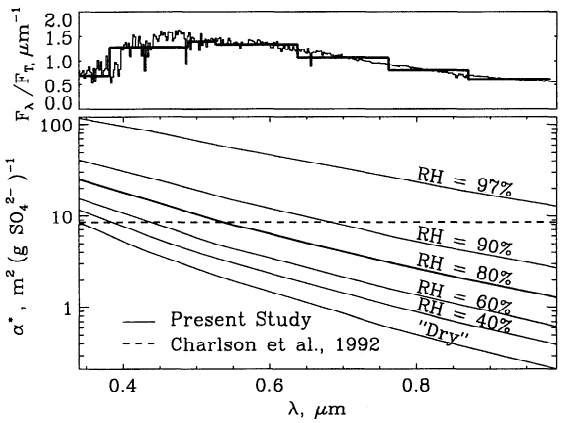

Figure 4. Scattering efficiency as a function of wavelength for ammonium sulfate. The dry particle radius (0.096 μm) was chosen such that the average α^* equals the *Charlson et al.* [1992] $\alpha^*_{\lambda=0.55\mu m}$ value of 8.5 m^2 g$(SO_4^{2-})^{-1}$ (dashed line) at RH = 80% (thick curve). For comparison, the α^* curves for other RH values are shown to indicate the high sensitivity of α^* to RH. Top panel shows the solar spectrum over the range employed in the scattering calculations divided by the solar constant, indicating the contribution of the solar spectrum toward the average α^* as a function of wavelength. The overlaying histogram represents the *Coakley et al.* [1983] spectral weights of the solar spectrum.

The phase function becomes increasingly peaked in the forward direction with increasing particle radius greater than approximately 0.05 μm [*Schwartz*, in press, 1995]. Because of the dependence of the phase function on particle size, β is also dependent on particle size.

An expression for evaluating the upscatter fraction for single scattering for a given SZA (θ_0) has been given by *Wiscombe and Grams* [1976] as an integral over scattering angle θ between limits defined by θ_0.

$$\beta(\theta_0) = \frac{1}{2\pi}\int_{\pi/2-\theta_0}^{\pi/2+\theta_0} P_{a,\lambda}(\theta)\sin\theta\cos^{-1}(\cot\theta_0\cot\theta)d\theta + \frac{1}{2}\int_{\pi/2+\theta_0}^{\pi} P_{a,\lambda}(\theta)\sin\theta d\theta \quad (9)$$

The dependence of β on θ_0 and particle radius R is examined in Figure 5. For the Sun at the horizon ($\mu_0 = 0$) the upscatter fraction attains its maximum value 0.5, independent of R, because of symmetry. Note that for large SZA's a substantial contribution to upscatter fraction results from scattering in the forward hemisphere; this is why upscatter fraction, not backscatter fraction, is the quantity pertinent to climate forcing. For the Sun increasingly close to the zenith, the predominant forward scattering of larger particles causes β to decrease, and particle size becomes increasingly important in determining the magnitude of the upscatter fraction.

To determine the forcing at a given location, it is necessary to evaluate the scattering integrated over a diurnal cycle, which integration necessarily involves large SZA. For illustrative purposes, the diurnal average upscatter fraction for ammonium sulfate for several latitudes and three dates (spring, summer, winter) is shown in Figure 6 as a function of the wet particle radius. The diurnal (24-hour) average β is,

$$<\beta>=\frac{\int_0^{24} F(\mu_0(t))\beta(\mu_0(t))dt}{\int_0^{24} F(\mu_0(t))dt}; \quad (10)$$

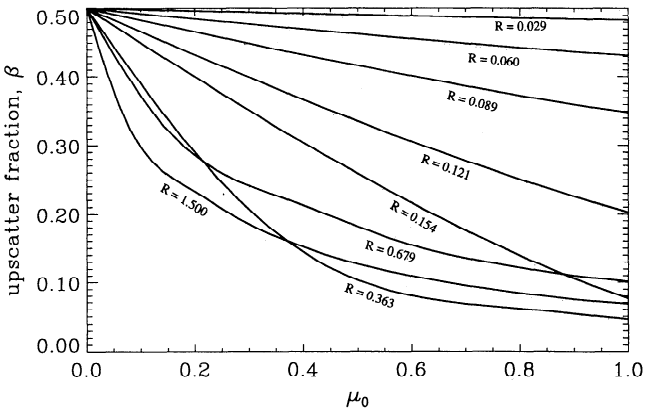

Figure 5. Dependence of upscatter fraction β on the cosine of the solar zenith angle, μ_0 and particle radius R (μm) at a wavelength $\lambda = 0.55$ μm and a refractive index of 1.4.

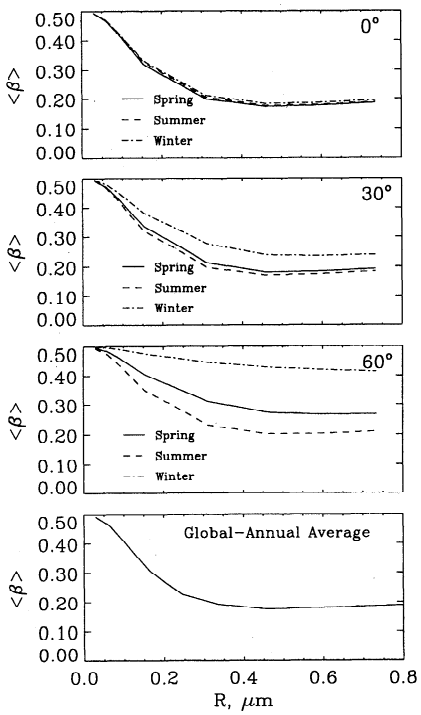

Figure 6. Diurnal (24-hour) average upscatter fraction $< \beta >$ for $(NH_4)_2SO_4$ averaged over the solar spectrum, for three seasons and several latitudes (°N) as a function of particle radius. Here winter = December 21, spring = March 21, and summer = June 21. The bottom panel represents the global-annual average $< \beta >$.

here $F(\mu_0)$ is taken as $\cos\theta_0$. As seen in Figure 6, the diurnal average upscatter fraction approaches 0.5 for small particle radii at all latitudes and seasons since, as noted above (Figure 5), the scattering phase function becomes symmetric in the forward and backward direction in the small particle limit. For all particle sizes there is very little variation in $< \beta >$ with season at the equator. At higher latitudes the variation with season is greater because of the greater seasonal differences in SZA. Note also that the magnitude of $< \beta >$ is greater at higher latitudes, suggesting a possible greater aerosol forcing at high latitudes resulting from this latitudinal dependence of upscatter fraction. We return to this point later. Also shown is the radius dependence of the global and annual average upscatter fraction over the illuminated hemisphere for a uniformly distributed aerosol, again showing the decrease in upscatter fraction with increasing particle radius.

3.3. Normalized Forcing

We now combine these several factors to obtain the normalized forcing. As with upscatter fraction this quantity is a function of SZA and particle radius. In order to relate normalized forcing to the microphysical properties of sulfate aerosol, we display this quantity as a function of particle dry radius for various values of the RH, as shown in Figure 7 for $(NH_4)_2SO_4$; the figures for the other compositions are similar. Several features of these plots should be noted. First there is a maximum

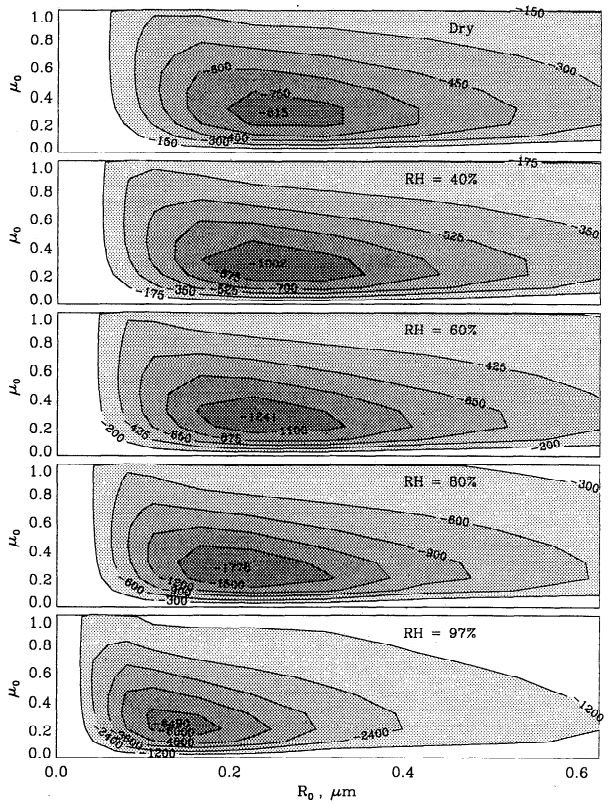

Figure 7. Instantaneous normalized clear-sky radiative forcing (ΔG) W g^{-1}(SO_4^{2-}) for $(NH_4)_2SO_4$ as a function of dry particle radius and $\mu_0 = \cos(\theta_0)$ for several relative humidities.

in the normalized forcing at any given RH and SZA that is due in part to the characteristic maximum in α^* as a function of radius noted in conjunction with Figure 3 (For simplicity we refer to the maximum in the magnitude of the normalized forcing as a maximum in normalized forcing, despite the fact that the quantity is negative). The dry radius that corresponds to the maximum forcing is about 0.25 μm for the dry particle (actual radius), decreasing with increasing RH to about 0.15 μm, as the actual radius becomes larger for a given dry radius.

It may be noted also that for any dry radius there is a maximum in forcing as a function of SZA. This maximum occurs not at the zenith, where the incident flux is the greatest, but at quite large SZA ($\mu_0 \approx 0.25$, corresponding to SZA $\approx 75°$). This displacement can be interpreted as the interworking of several factors. Because the calculation is based on an aerosol of low optical depth (optically thin), the effective path length for scattering varies as sec(θ_0), effectively canceling the cos(θ_0) dependence in incident solar flux. Consequently, the increase in normalized forcing with increasing SZA is due to the SZA dependence of β, Figure 5. Why then is SZA corresponding to a maximum ΔG not at $\mu_0 = 0$ ($SZA = 90°$), as is the case with β? Because ultimately, at high SZA the incident flux is decreased by Rayleigh scattering.

A further key feature displayed in Figure 7 is the strong increase in the magnitude of the normalized forcing with increasing RH. This RH dependence results largely from the RH dependence of α^*, Figure 3; that is, the factor $\mathcal{F}(RH)$ in the notation of *Charlson et al.* [1992]. It may be seen that this increase is relatively slight (about 20%) for supersaturated $(NH_4)_2SO_4$ at RH = 40% versus the dry material, but increases quite markedly as the material swells with increasing RH (Figure 1). The strong dependence of forcing on RH makes it crucial that this influence be accurately represented in evaluating radiative forcing by sulfate aerosols.

Further quantities important to understanding the direct forcing are averages of the normalized forcing over various geophysical variables. Figure 8 displays the dependence of diurnal (24-hour) average normalized forcing on particle size and RH for a specific latitude (30°N) and date (June 21), explicitly showing also the dependence on chemical composition. The dependencies of forcing on size and RH is similar for the several compositions. Again, a characteristic maximum in forcing is exhibited as a function of particle size, reflecting mainly the maximum in α^*. The strong dependence on RH should also again be noted.

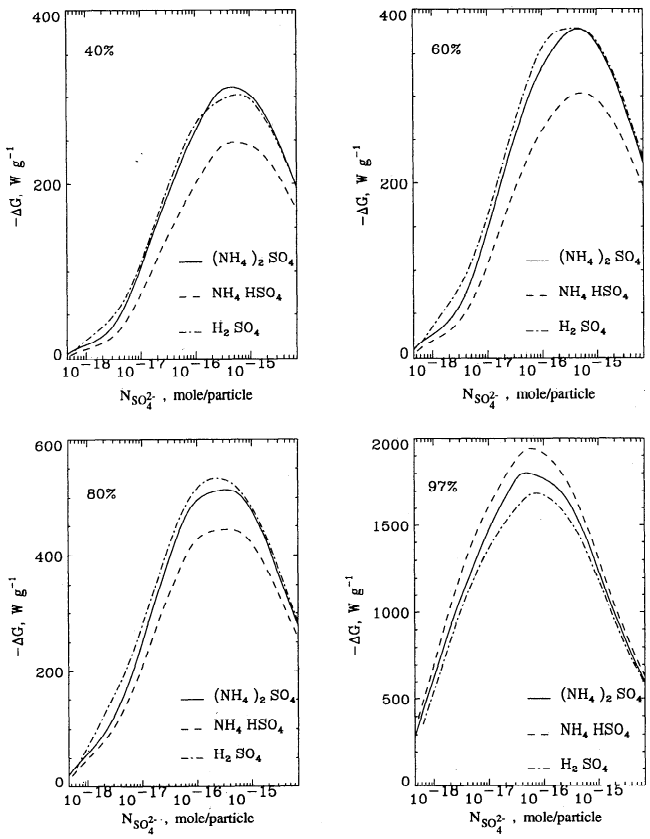

Figure 8. Magnitude of the diurnal (24-hour) normalized clear-sky aerosol forcing as a function of particle size (amount of sulfate in the particle, $N_{SO_4^{2-}}$) for several relative humidities and particle compositions at 30°N latitude, for June 21. For corresponding particle dry radius, see Figure 3.

Figure 9 shows the variation of the normalized diurnal-average forcing with season and latitude for several values of particle wet radius. This figure is particularly pertinent to displaying the influence of β in displacing the maximum normalized forcing to large SZA. At high latitude the average SZA is greater than at lower latitudes, resulting in an increase in the magnitude of the forcing. This can be demonstrated by comparing the several curves for spring, since at the spring equinox the length of the day is 12 hours at all latitudes. Therefore for this date the variation in diurnal average forcing with latitude depends not on length of day but only on μ_0. At small radius (R = 0.029 μm) β is insensitive to μ_0 (Figure 5), so β does not greatly influence the latitudinal dependence on the forcing. Since half the scattered photons are scattered into the upward direction at all SZA's, there is no increase in ΔG with increasing SZA, and ΔG falls off from equator toward higher latitude as a consequence of the enhanced Rayleigh scattering at higher latitudes due to increased SZA. However, with increasing R, the increase in β with increasing SZA exerts its influence, displacing the maximum forcing to higher latitudes. Of course at higher latitudes length of day also exerts a strong influence in the magnitude of normalized forcing, as has been noted previously [*Hunter et al.*, 1993]. Finally, note that as a function of radius the magnitude of the normalized forcing reaches a maximum and then becomes smaller at the larger particle radius.

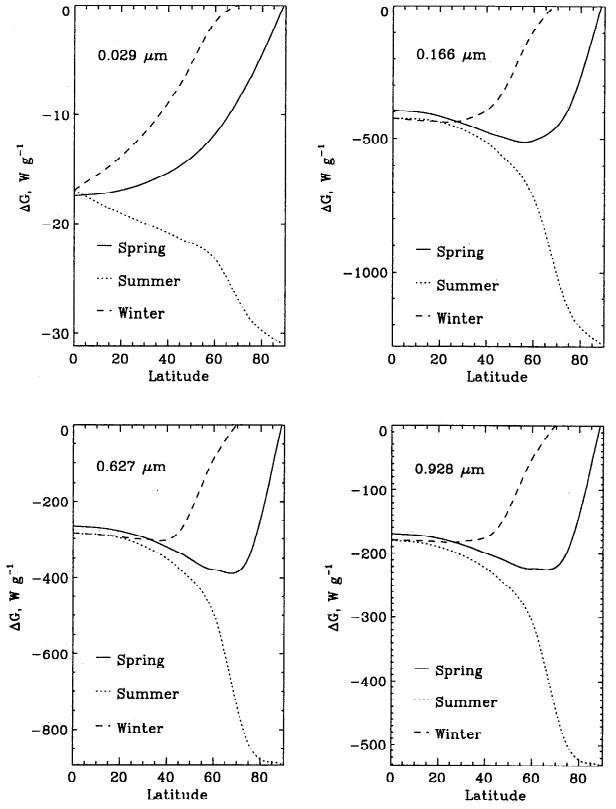

Figure 9. Seasonal and latitudinal dependence of diurnal (24-hour) average normalized clear-sky aerosol forcing for $(NH_4)_2SO_4$ at RH = 80% for several actual particle radii.

This is directly related to the radius dependence of the scattering efficiency. Figure 9 shows that season and latitude are strong indicators in determining the aerosol forcing as a consequence of the influence of these variables on SZA and in turn β. Since anthropogenic aerosols are nonuniformly distributed by latitude and season, these latitudinal and seasonal dependences of normalized forcing may enhance or diminish the actual aerosol forcing relative to calculations that assume a uniformly distributed aerosol.

4. Discussion

Figure 10 shows the global and annual average normalized forcing as a function of particle dry radius and RH. In computing this average, we treat the aerosol as uniformly distributed over the illuminated hemisphere (this assumption is not required; any other distribution could be readily treated). As noted previously in Figures 7 and 8, a maximum in normalized forcing is exhibited as a function of particle dry radius, with the value of the radius that corresponds to this maximum decreasing slightly with increasing RH. Again, also the strong RH dependence is manifest.

As noted in the introduction, the forcing for an actual aerosol needs to be evaluated by integrating the radius dependent forcing over the size distribution of the aerosol. Here for illustration, we carry out such an evaluation using four different size distributions under the assumption that the aerosol is uniformly comprised of $(NH_4)_2SO_4$ at RH = 80%. These four distributions, shown in the top panel of Figure 10, correspond to measurements of marine and continentally influenced

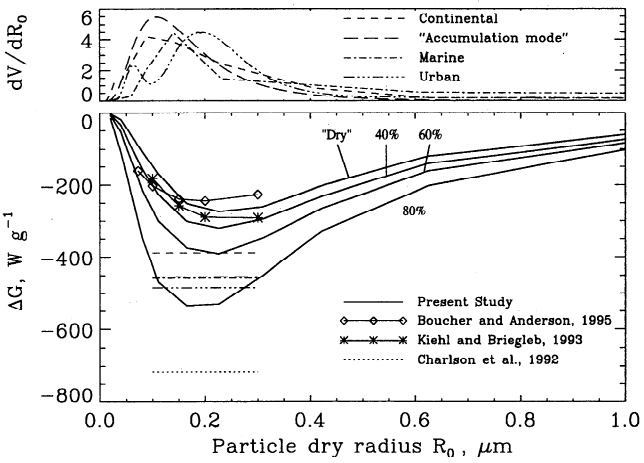

Figure 10. Normalized clear-sky global annual average forcing ammonium sulfate aerosol for a hypothetical clear-sky planet as a function of particle dry radius for several RH. Also shown are the normalized clear-sky forcings of *Boucher and Anderson* [1995] and *Kiehl and Briegleb* [1993] corresponding to the values of forcings given in their Figure 7 and Figure 3, respectively, with σ_g = 1.4. The several horizontal lines represent the normalized forcing of *Charlson et al.* [1992] and the clear-sky global annual average normalized forcings corresponding to the several size distributions displayed in the top panel, all for RH = 80%.

aerosol [*Hoppel et al.*, 1990], urban aerosol sulfate [*John et al.*, 1990], and the classical accumulation mode distribution of *Whitby* [1978] (volume size distribution with $r_g = 0.15$ μm and $\sigma_g = 0.57$). The global hemispheric average normalized forcing at RH = 80% for these four distributions is shown in the bottom panel of Figure 10. The spread among the several distributions is about 20%.

Figure 11 shows the global hemispheric average normalized forcing as a function of RH for the several size distributions given in Figure 10 (the marine distribution is not shown since the normalized forcings are almost identical to those for the accumulation mode distribution) under the assumption that the aerosol is uniformly comprised of the indicated sulfate species. The forcing is computed by integrating over SZA and then over particle size. Note that the spread among the several distributions and compositions is about ±26% for low RH decreasing to ±13% at RH = 97%. Of course, for each of these distributions and compositions, RH is a major factor, especially at RH > 80%.

In order to compare present estimates of forcing with those of previous investigators, Figure 10 also shows the normalized clear-sky forcings evaluated from data presented by *Charlson et al.* [1992], *Kiehl and Briegleb* [1993], and *Boucher and Anderson* [1995]. Comparison of the normalized global and annual forcings in Figure 10 shows that the present results are intermediate between those of earlier investigators, less than the value obtained with the box model of *Charlson et al.* [1992] and greater than the distributed aerosol forcing calculations of *Kiehl and Briegleb* [1993] and *Boucher and Anderson* [1995]. We briefly discuss possible reasons for these differences.

In comparing to the normalized forcing of *Charlson et al.* [1992], we explicitly compare the forcing at 80% RH, which corresponds [*Charlson et al.*, 1991] to the RH enhancement factor $\mathcal{F} = 1.7$ employed in the 1992 box model calculation, for which the normalized forcing is -715 W $g(SO_4^{2-})^{-1}$. In contrast for the several size distributions and compositions at RH = 80%, we obtain a normalized clear-sky forcing of -450 ± 50 W $g(SO_4^{2-})^{-1}$ (Figures 10 and 11), about 40% lower than the *Charlson et al.* [1992] value. As noted above, *Kiehl and Briegleb* [1993] attributed the high forcing of *Charlson et al.* [1992] to the application in that calculation of a constant, high value of scattering efficiency, α^*, that corresponded to 0.55 μm, to the entire solar spectrum, whereas this quantity falls off strongly with wavelength, Figure 4. To some extent this criticism is justified. However, there is a compensating factor that to some degree offsets a correction based solely on the wavelength dependence of α^*, which arises from the wavelength dependence of Rayleigh scattering ($\sim \lambda^{-4}$) relative to that of aerosol scattering ($\sim \lambda^{-1}$). Specifically, Rayleigh scattering, which reduces the effect of the aerosol scattering, exerts a lesser reduction at longer wavelengths than at shorter wavelengths. In any event, comparison of the *Charlson et al.* [1992] value of 8.5 m^2 $g(SO_4^{2-})^{-1}$ with the values of α^* in Figure 3 shows that the value of 8.5 m^2 $g(SO_4^{2-})^{-1}$ is exceeded for R_0 between 0.09 μm and 0.4 μm, which range encompasses the great majority of the aerosol volume for the several distributions given in Figure 10. Likewise integration of α^* over the several size distributions in Figure 10 gives values ranging from 9.3 to 11.7 m^2 $g(SO_4^{2-})^{-1}$, supporting, if anything, a value of α^* greater than the value employed in the box model evaluation of *Charlson et al.* [1992]. It should be reiterated that the values of α^* given in Figure 3 represent integrations taken over the visible spectrum indicated in Figure 4.

A second possible reason for the departure from the *Charlson et al.* [1992] normalized forcing is in the upscatter fraction β, which those investigators had taken as a constant value of 0.29, which for $\alpha^* = 8.5$ m^2 $g(SO_4^{2-})^{-1}$ corresponds to $\alpha^*\beta = 2.46$ m^2 $g(SO_4^{2-})^{-1}$. Examination of Figures 5 and 6 shows that β decreases strongly with increasing R in the radius range pertinent to the size distributions of accumulation mode aerosols. The average value of β exceeds the *Charlson et al.* [1992] value of 0.29 for particle radius less than 0.3 μm, which at RH = 80% corresponds (Figure 1) to a dry radius of 0.2 μm. *Kiehl and Briegleb* [1993] suggested that there is a compensating effect of $\alpha^*\beta$ with increasing RH, wherein as α^* increases, β decreases. However, this does not appear to account for the discrepancy. Specifically, for the four size distributions shown in Figure 10, the quantity $\alpha^*\beta$ ranges from 2.45 to 2.79 m^2 $g(SO_4^{2-})^{-1}$ at RH = 80% throughout much of the pertinent range of dry radius and SZA, that is, somewhat greater than the value corresponding to the evaluation of *Charlson et al.* [1992]

Another possible factor that might give rise to a difference between the *Charlson et al.* [1992] treatment and the present calculation is the different way of

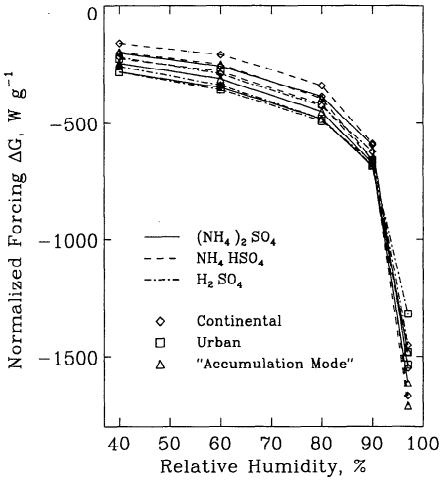

Figure 11. Relative humidity dependence of normalized global average clear-sky forcing for sulfate aerosol for the several dry size distributions shown in top panel of Figure 11; values for the marine distribution are not shown as they are indistinguishable from those for the accumulation mode distribution.

treating atmospheric transmission. In the present treatment, the atmospheric absorption outside the wavelength range of 0.3 to 1 μm was approximated to be complete, corresponding to $T_a = 0.69$, and the spectrally averaged transmission through the conservative Rayleigh scattering atmosphere was $T_R = 0.9$, for which the overall transmission factor $T_f = T_a T_R^2 = 0.56$. This transmission factor is essentially identical to that in the *Charlson et al.* [1992] approach, for which the molecular absorption and Rayleigh scattering was represented by a transmission factor of $T_f = T^2 = 0.58$. Hence this difference also cannot account for the discrepancy.

On the basis of these comparisons we conclude that the lower values for normalized forcing obtained here compared to that of *Charlson et al.* [1992] are not due to systematic differences in aerosol optical properties but rather, for reasons noted in the above paragraphs, are due to a more exact treatment of aerosol scattering by the doubling and adding radiative transfer method compared to the simple treatment via albedo enhancement by *Charlson et al.* [1992].

Comparison of the present results with those of *Kiehl and Briegleb* [1993] and *Boucher and Anderson* [1995] is somewhat more difficult for a number of reasons. In order to evaluate the corresponding quantity from those studies it is necessary to back calculate the normalized clear-sky direct forcing from the reported global annual mean average forcing and the anthropogenic sulfate loadings employed in the calculations. In both instances it was necessary to adjust the forcings to a cloud-free planet by means of the so-called cloud factor that takes into account the weighting of the contributions to global mean forcing from cloud-free and cloud-covered regions [*Boucher and Anderson*, 1995]. This weighting is necessary because aerosol forcing, although strongly reduced in a cloudy environment compared to cloud-free sky, is still appreciable (according to *Boucher and Anderson* [1995], about 25% as efficient in overall average). (Note that *Charlson et al.* [1992] assumed the forcing to be zero in the presence of clouds.) The parameters used to compute the clear-sky normalized forcing for the earlier studies to which the present results are compared are given in Table 2. In order to compare most closely to the present results, we present forcings from those studies for the lowest reported value of the geometric standard deviation in the particle radius distribution, $\sigma_g = 1.4$. It may be seen that the normalized forcings inferred in this way are substantially lower than the present results for RH = 80%, corresponding rather more closely to those for lower RH values, although the comparison is somewhat qualified because the global and annual mean forcings from the global distributions arise from the averaging over the individual grid cells, with their corresponding RH values (their average daytime RH for the lower troposphere is closer to 60 than 80%), rather than from the specific fixed RH values employed here. Also, complications arise because of variation of RH and surface albedo in these models with season, latitude, and region. Still, the present estimates appear systematically greater than those from *Kiehl and Briegleb* [1993] and *Boucher and Anderson* [1995]. Possible reasons for these differences include differences in treatment of the microphysics and radiation. For example, *Kiehl and Briegleb* [1993] used an empirical treatment for RH dependence for aerosol scattering properties rather than one based on the deliquescence properties of the specific sulfate compounds together with Mie theoretical treatment of scattering cross section and upscatter fraction as was employed here. Also, *Boucher and Anderson* [1995] used a radiation transfer code that divides the spectral interval into only two bins and thus may not adequately represent the spectral dependence of scattering efficiency and upscatter fraction.

Recently, *Haywood and Shine* [1995] reported results of a Mie scattering calculation for a particular assumed aerosol size distribution, namely, lognormal number distribution, with mode radius 0.05 μm and $\sigma_g = 2.0$. On the basis of this calculation they suggest that the several parameters in (1) be revised in the direction of reduced forcing: $\overline{\beta} = 0.21$; $\alpha^* = 6.8$ m^2 g^{-1} at 70% RH. Apparently, the rather low value of $\overline{\beta}$ results from *Haywood and Shine's* [1995] use of a particle volume distribution that is heavily skewed to large radius (volume mean radius 0.27 μm) as a consequence of the high geometric standard deviation of the number

Table 2. Summary of the Parameters Used for Computing the Clear-sky Normalized Forcings for Previous Studies With Which the Present Results are Compared

Reference	$B_{SO_4^{2-}}$, mg m^{-2}	CF^*	A_c	σ_g^+
Charlson et al. [1992]	4.0	n.a.	0.61	n.a.
Kiehl and Briegleb [1993$^{\mp}$]	1.77	0.64	0.62	1.4
Boucher and Anderson [1995]	2.32	0.61	0.53	1.4

(*) The cloud factor (CF) is defined as the ratio of $\Delta G_{all-sky}$ to $\Delta G_{clear-sky}$. CF relates to the fractional cloud cover (A_c) through the relation [*Boucher and Anderson*, 1995] $\Delta G_{all-sky} = \Delta G_{clear-sky}(1 - A_c) + \Delta G_{cloud} A_c$.
(+) σ_g denotes the geometric standard deviation of a log-normal size distribution.
($\mp$) as reported by *Boucher and Anderson* [1995].

distribution employed. On the basis of observed volume distributions of sulfate aerosol such as those shown in Figure 10, we see no justification for the use of such a large geometric standard deviation for accumulation mode sulfate and suggest that the value of $\overline{\beta}$ proposed by *Haywood and Shine* [1995] may be artificially low. In any event, the sensitivity to choice of size distribution suggests the necessity of carrying out integrations over measured size distributions rather than assumed canonical size distributions if estimates of normalized forcing are to be improved.

5. Conclusion

The influence of microphysical and chemical properties of anthropogenic sulfate aerosol on radiative forcing of climate by direct scattering of shortwave radiation has been assessed by radiative transfer calculations based on Mie scattering properties of the aerosol. The controlling quantities are mass scattering efficiency and upscatter fraction. The joint influence of these quantities is accurately and conveniently represented by the normalized clear-sky forcing, the quotient of the direct forcing by the column integral of the aerosol sulfate mass. Normalized forcing can be evaluated locally and instantaneously, as a function of solar zenith angle, or as an average over time and/or space as desired. The key quantities influencing normalized forcing are particle size and index of refraction, which are determined by the composition and size distribution of the dry aerosol and by relative humidity. Normalized forcing increases strongly with increasing RH, especially at RH greater than 80%, as a consequence of accretion of water mass by the hygroscopic material. The normalized forcing exhibits a (negative) maximum for dry particle radius 0.15 to 0.3 μm, decreasing with increasing RH, mainly as a consequence of the size dependence of the scattering efficiency. The maximum normalized forcing occurs at large SZA (about 75°), as a consequence of the large contribution to upscatter fraction from forward scattered radiation. Because of this zenith angle dependence, normalized forcing increases somewhat with increasing latitude. Normalized forcing for an arbitrary aerosol size distribution is readily evaluated as an integral over the radius dependence of this quantity. The magnitude of normalized forcing varies somewhat for representative aerosol size distribution and composition, suggesting the utility of evaluations of the radiative influence of grounded in Mie scattering theory making use of measured or modeled aerosol size distributions and explicitly accounting for the RH dependence of the scattering.

Note added in proof. Subsequent to submission of this paper a paper entitled "Sensitivity of Direct Climate Forcing by Atmospheric Aerosols to Aerosol Size and Composition" by C. Pilinis, S. N. Pandis, and J. H. Seinfeld was published (J. Geophys. Res. 100, 18739-18754, 1995). That paper presented findings regarding the dependence of forcing on solar zenith angle and relative humidity that are qualitatively similar to those of the present paper.

Acknowledgments. We thank James E. Hansen and Larry D. Travis for supplying the Mie scattering model and the Doubling-Adding multiple scattering routine for calculating the scattering phase matrices and the radiative forcing. This research was supported by the Environmental Sciences Division of the U.S. Department of Energy (DOE) as part of the Atmospheric Radiation Measurement Program and was performed under the auspices of DOE under contract DE-AC02-76CH00016.

References

Boucher, O., and T. L. Anderson, GCM assessment of the sensitivity of direct climate forcing by anthropogenic sulfate aerosols to aerosol size and chemistry, *J. Geophys. Res., in press*, 1995.

Charlson, R. J., J. Langner, and H. Rodhe, Sulfate aerosol and climate, *Nature*, *348*, 22, 1990.

Charlson, R. J., J. Langner, H. Rodhe, C. B. Leovy, and S. G. Warren, Perturbation of the northern hemisphere radiation balance by backscattering from anthropogenic sulfate aerosols, *Tellus*, *43AB*, 152–163, 1991.

Charlson, R. J., S. E. Schwartz, J. M. Hales, R. D. Cess, J. A. Coakley, J. E. Hansen, and D. J. Hofmann, Climate forcing by anthropogenic aerosols, *Science*, *255*, 423–430, 1992.

Coakley, J. A., R. D. Cess, and F. B. Yurevich, The effect of tropospheric aerosols on the earth's radiation budget: A parameterization for climate models, *J. Atmos. Sci.*, *40*, 116–138, 1983.

Forgan, B. W., Aerosol optical depth, *Baseline Atmospheric Program 1985*, edited by B. W. Forgan, and P. J. Fraser, pp. 50–56, Dep. Sci./Bur. of Meteorol. and Commonwealth Sci. and Ind. Res. Org./Div. of Atmos. Res., Australia, 1987.

Garland, J., Condensation on ammonium sulphate particles and its effect on visibility, *Atmos. Environ.*, *3*, 347–354, 1969.

Hansen, J., and L. Travis, Light scattering in planetary atmospheres, *Space Sci. Rev.*, *16*, 527–610, 1974.

Haywood, J. M., and K. P. Shine, The effect of anthropogenic sulfate and soot aerosol on the clear sky planetary radiation budget, *Geophys. Res. Lett.*, *22*, 603–606, 1995.

Hegg, D., R. Ferek, and P. Hobbs, Light scattering and cloud condensation nucleus activity of sulfate aerosol measured over the northeast atlantic ocean, *J. Geophys. Res.*, *98*, 14,887–14,894, 1993.

Hoppel, W. A., J. W. Fitzgerald, G. M. Frick, and R. E. Larson, Aerosol size distributions and optical properties found in the marine boundary layer over the Atlantic Ocean, *J. Geophys. Res.*, *95*, 3659–3686, 1990.

Hunter, D. E., S. E. Schwartz, R. Wagener, and C. M. Benkovitz, Seasonal, latitudinal, and secular variations in termperature trend: Evidence for influence of anthropogenic sulfate, *Geophys. Res. Lett.*, *20*, 2455–2458, 1993.

Intergovernmental Panel on Climate Change (IPCC), World Meteorological Office, United Nations Environmental Programme, *Radiative Forcing of Climate Change. The 1994 Report of the Scientific Assessment Working Group of IPCC, Summary for Policymakers.*, World Meteorol. Org., Geneva, 1994.

John, W., S. M. Wall, J. L. Ondo, and W. Winklmayr, Modes in the size distributions of atmospheric inorganic aerosol, *Atmos. Environ.*, *24*, 2349–2359, 1990.

Kaufman, Y. J., and B. N. Holben, Hemispherical backscattering by biomass burning and sulfate particles derived from sky measurements, *J. Geophys. Res.*, in press, 1995.

Kiehl, J. T., and B. P. Briegleb, The relative roles of sulfate aerosols and greenhouse gases in climate forcing, *Science*, *260*, 311–314, 1993.

Penner, J. E., R. E. Dickinson, and C. A. O'Neill, Effects of aerosol from biomass burning on the global radiation budget, *Science*, *256*, 1432–1433, 1992.

Penner, J. E., R. J. Charlson, J. M. Hales, N. S. Laulainen, R. Leifer, T. Novakov, J. Ogren, L. F. Radke, S. E. Schwartz, , and L. Travis, Quantifying and minimizing uncertainty of climate forcing by anthropogenic aerosols, *Bull. Am. Meteorol. Soc.*, *75*, 375–400, 1994.

Rood, M. J., M. A. Shaw, T. V. Larson, and D. S. Covert, Ubiquitous nature of ambient metastable aerosol, *Nature*, *337*, 537–539, 1989.

Schwartz, S. E., Are global cloud albedo and climate controlled by marine phytoplankton?, *Nature*, *336*, 441–445, 1988.

Schwartz, S. E., The whitehouse effect: Shortwave radiative forcing of climate by anthropogenic aerosols, *J. Aerosol Sci.*, in press, 1995.

Tang, I. N., and H. R. Munkelwitz, Aerosol growth studies, iii, ammonium bisulfate aerosols in a moist atmosphere, *J. Aerosol Sci.*, *8*, 321–330, 1977.

Tang, I. N., and H. R. Munkelwitz, Water activities, densities, and refractive indices of aqueous sulfates and sodium nitrate droplets of atmospheric importance, *J. Geophys. Res.*, *99*, 18,801–18,808, 1994.

Taylor, K. E., and J. E. Penner, Response of the climate system to atmospheric aerosols and greenhouse gases, *Nature*, *369*, 734–737, 1994.

Twomey, S., Optics of individual aerosol particles, *in Atmospheric Aerosols, pp. 199-217*, Elsevier, New York, 1977.

Twomey, S., M. Piepgrass, and T. L. Wolfe, An assessment of the impact of pollution on gobal cloud albedo, *Tellus*, *36B*, 356–366, 1984.

Weast, R. P., and M. J. Astle, *Handbook of Chemistry and Physics*, The Chemical Rubber Co., Ohio, 63 ed., 1982.

Whitby, K. T., The physical characteristics of sulfur aerosols, *Atmos. Environ.*, *12*, 135–159, 1978.

Wigley, T. M. L., and S. C. B. Raper, Implications for climate and sea level of revised IPCC emissions scenarios, *Nature*, *33*, 293, 1992.

Wiscombe, W., and G. Grams, The backscattered fraction in two-stream approximations, *J. Atmos. Sci.*, *33*, 2440–2451, 1976.

S. Nemesure, S. E. Schwartz, R. Wagener, Environmental Chemistry Division, Brookhaven National Laboratory, Bldg. 426, Upton, NY 11973-5000.
(email: seth@bnl.gov; ses@bnl.gov; wagener@bnl.gov)

(Received May 24, 1995; revised September 5, 1995; accepted September 5, 1995.)